

Degradation of Polymer Coating Systems Studied by Positron Annihilation Spectroscopy. 1. UV Irradiation Effect

H. Cao, Renwu Zhang, C. S. Sundar,[†] Jen-Pwu Yuan, Y. He, T. C. Sandreczki,* and Y. C. Jean*

Department of Chemistry, University of Missouri—Kansas City, Kansas City, Missouri 64110

B. Nielsen

Department of Applied Science, Brookhaven National Laboratory, Upton, New York 11973

Received February 23, 1998; Revised Manuscript Received June 11, 1998

ABSTRACT: The degradation of polymer coating systems due to UV irradiation is studied using positron annihilation spectroscopy. Doppler broadened spectra of positron annihilation are measured as a function of slow positron implantation energy in a series of polymer coating systems which were exposed to UV irradiation for up to 2000 h. The *S* parameters from the Doppler broadened energy spectra vs positron energy show an increase at very low positron energy (<575 eV) and then a decrease to about 8 keV, followed by a slight increase up to 50 keV. The UV irradiation systematically decreases the *S* parameter as a function of exposure duration. The significant *S* parameter decrease is interpreted as the degradation of polymers and the change of the sub-nanometer defect profiles due to UV irradiation. These interpretations are supported by the data from the atomic force microscope, UV absorption, Fourier transform infrared, and profilometry measurements.

Introduction

A coating system is a multilayered structure consisting of a topcoat, a primer, and a surface treatment next to the substrate, which is usually a metal or structural material.¹ Each layer of the coating system performs several special functions and interacts with the other layers to achieve the main desired attributes of longevity, corrosion protection, and good cosmetic appearance. For example, in present-day aluminum-skinned aircraft, the topcoat and primer are mainly comprised of organic polymers, such as polyurethane for the topcoat and epoxy for the primer, with solvent and pigment additives.² The primer and surface treatment contain metallic oxides, such as chromates. The topcoat layers (~ μm) provide appearance and protection against environmental erosion and mechanical abrasion. The surface treatment layer (~10 nm) provides passivation of the metal surface, optimizes topography for primer adhesion, and inhibits corrosion.³

Durability is a primary concern for coating systems.⁴ Environmental degradation from moisture, light, weather, and fluids reduces the service lifetime.⁵ There is limited understanding of the cause of low durability in most coating systems.^{4,5} Existing methods of assessing durability and degradation are chiefly macroscopic approaches, measuring mechanical properties such as adhesion, hardness, pulling strength, etc. Most knowledge of coating degradation and failure is based on these evaluations of performance.⁴ However, the origins, mechanisms, and progression of degradation are not yet fully ascertained for coating systems. Only recently spectroscopic and physical methodologies have been used to investigate the underlying course of coating degradation.^{6,7}

Analytical techniques which monitor the physico-chemical changes that occur during degradation include

spectroscopy methods, such as Fourier transform infrared (FTIR) and Raman spectroscopy,^{7,8} where configurational and conformational variations are detectable. Resonance methods, such as nuclear magnetic resonance (NMR)⁹ and electron spin resonance (ESR),¹⁰ can detect local environmental changes due to photodegradation at the molecular level. Changes in chemical properties are correlated with changes in physical properties. Characterization of physical changes during the degradation of paints has been pursued by scattering and microscopy methods,¹¹ such as scanning electron microscopy (SEM), transmitting electron microscopy (TEM), atomic force microscopy (AFM), scanning tunneling microscopy (STM), and X-ray, electron, neutron, and ion diffractions. Each of these analytical techniques has its advantages and shortcomings in structural determination and elemental sensitivity. A multitechnique approach appears to be very important. While X-ray diffraction and small-angle neutron scattering (SANS) are commonly used to measure defect dimensions, they are limited to the larger dimensions (>nm). On the other hand, atomic probes, SEM, STM, and AFM are powerful detectors of static defects near the surface. One important approach is to study the very origins of physical defects during the degradation process: i.e., from the Å (0.1 nm) level and a 10^{-9} s time scale.

Because the degradation process is critical to topcoat layers where chemical, physical, and mechanical changes begin, surface analysis becomes vital to the understanding of coating durability problems. Surface techniques, such as X-ray photoelectron spectroscopy (XPS), secondary ion mass spectroscopy (SIMS), and scanning Auger microscopy (SAM),¹¹ can provide useful information about chemical states and electronic properties. Yet even with all these efforts, degradation mechanisms are not fully understood. There is incomplete fundamental understanding of defect properties and their interrelationships from the topmost layers of paint through all coating layers and their interfaces. The concept of

[†] On leave. Current address: Materials Science Division, Indira Gandhi Centre for Atomic Research, Kalpakkam, Tamil Nadu, 603102, India.

correlating the physical defects, such as atomic vacancy, free volume, holes, voids, interfaces, and surfaces, with the molecular structure and chemical defects, is the central idea in this study. In this paper, we report the result of using an innovative physical technique, positron annihilation spectroscopy (PAS),¹² to investigate physical defects at the atomic level of coating systems as a function of environmental and mechanical changes and molecular modifications.

PAS is a special nondestructive evaluation (NDE) technique for materials characterization which uses the positron (antielectron). Positron–electron annihilation γ -rays reveal useful information about the electronic and defect properties of materials under study. The unique repulsive force between the positron and the ion cores of materials makes the positron ideal for probing defects at the atomic and molecular levels. In recent years, PAS was developed as a useful tool to probe the microscopic properties of polymeric materials.¹³ One of the great successes in this line of research is the direct determination of polymer free-volume and hole properties at an atomic scale (0.2–2 nm). Most existing PAS studies emphasize the bulk of polymers in measuring positron annihilation lifetime (PAL). In this work, we use another method of positron annihilation radiation, Doppler broadening of energy spectra (DBES), coupled with a slow positron beam to examine the defect profile near the surface.

Current positron beam spectroscopy uses a variable positron energy beam (from kT to several MeV) coupled with positron annihilation lifetime and momentum density measurements and is capable of probing defect profiles from the topmost layer (~ 0.1 nm) of the surface down to the bulk layers (several μm).¹⁴ Recently, a positron study of a paint surface has shown a distinct difference in positron annihilation signals from weathered and unweathered samples with and without pigments.¹⁵

In addition to the use of a combination of PAS techniques, we recognize the importance of using more conventional techniques to provide complete physical and chemical information about corrosion and degradation mechanisms for coating systems. In this work, we also employed various traditional methods such as ESR, ATR-FTIR, profilometry, and AFM to provide more complete information about chemical and physical properties of the same coating samples.

Experiments

The samples investigated are of particular interest in aircraft applications. They were prepared from raw materials provided by Deft Co. which follow the military specifications: MIL-P-23377G-Class C for the primer and MIL-C-85285B or MIL-C-36375 for the topcoat. The topcoat material was a polyurethane-based polymer, and the primer was an epoxy-based polymer. Both materials contain pigment, such as TiO_2 (ca. wt, 18%; particle size, 0.2–2 μm), colorants, and other additives. Both topcoat and primer materials were mixed in organic solvent. Primers were spin-coated onto an aluminum plate (2024-T3 alloy). After 20 h when the primers were completely dried, the topcoats were spin-coated onto the prepared primers. The final prepared coating systems were then stored in a drybox prior to UV irradiation. Pure urethane polymer was prepared mixing N-3300 diisocyanate and 670A-80 polyester polyol (Bayer Chemical) in the equivalent ratio 1.05:1, and then spin-coated onto Al. TiO_2 powders were purchased from Aldrich Chemicals (Milwaukee, WI).

Controlled UV irradiations were performed in a Q-panel environmental chamber (Cleveland, OH). The UV wavelength was 340 nm, and the chamber temperature was controlled at

45 ± 1 °C with a relative humidity below ambient, due to the elevated temperature. Two sets of samples were made: one directly facing the UV light and the other without the light. The samples without the light exposure were also used in the positron experiments to detect degradation effects due to thermal annealing. They show insignificant changes in S parameters compared with the unexposed original coating systems. The UV-irradiated coating systems were stored in a dark box to prevent further light exposure before the positron experiments.

The thickness of the coating systems was measured using a profilometer (Tencor 10, Advanced Surface Technology, Cleveland, OH). The total thickness of the prepared coating systems was measured at 37.6 μm , consisting of a 23.4 μm topcoat and a 14.2 μm primer. The thickness scans for both primer and coating (primer + topcoat) on Al substrate are shown in Figure 1. The density of the coating systems was determined to be 1.50×10^3 kg/m³ from weight and volume measurements of the same coating systems after dissolving Al in diluted hydrochloric acid.

For DBES experiments, a slow positron beam at Brookhaven National Labs was used.¹⁴ The vacuum in the sample chamber was approximately 10^{-6} and 10^{-8} Torr at high and low temperatures, respectively. The DBES spectra were recorded at room temperature (23 °C) as a function of positron energy from ca. 0 to 50 keV. The slow positrons were generated with a 15 mCi of ^{22}Na , moderated by the use of W foils and electromagnetically transported to polymer samples. The DBES spectra were recorded using an HP Ge Detector (EG&G Ortec with 35% efficiency and energy resolution of 1.5 keV at the 512 keV peak) at a counting rate of approximately 1500 cps. The total number of counts for each DBES spectrum was 0.3–1.0 million.

The obtained DBES spectra were characterized by an S parameter, defined as a ratio of integrated counts between $E_1 = 509.41$ and $E_2 = 512.59$ keV (the central part) to the total counts after the background was properly subtracted expressed as follows:

$$S = \frac{\sum_{E_1}^{E_2} N(E_i)}{\sum_{E_i=0}^{\infty} N(E_i)} \quad (1)$$

Since the S parameter represents the relative value of the low-momentum part of positron–electron annihilation radiation, it is sensitive to the change of the positron and positronium (Ps) states due to microstructural changes.^{12,14} When the positron and Ps are localized in a hole or free volume with a finite size, the observed S parameter is a measure of the momentum broadening according to the uncertainty principle: a larger hole results in a larger S parameter value. The S parameter has been successfully used in the detection of defect profiles in semiconductors at a high sensitivity.¹⁴ Figure 2 schematically shows the definition of the S parameter in a DBES spectrum.

The UV–visible absorption spectra of coating systems were performed using the Cary-1 Spectrometer from wavelength 240 to 700 nm. The linear extinction coefficient (ϵ) of 340 nm in the coating systems was found to be $0.23 \mu\text{m}^{-1}$, as calculated from the spectra obtained at the samples with different thicknesses on quartz. The UV absorbance in the coating systems follows a simple exponential decay according to Beer's law. It is observed that UV irradiation penetrates through a few micrometers of the paint samples studied here.

The vibrational spectra for both un-irradiated and UV-irradiated coating samples were recorded using an FTIR (Nicolet Magna IR 5600 under an attenuated total reflectance, ATR, mode) to detect any change near the surface of the paints due to UV irradiation. Figure 3 shows the absorbance spectra for both un-irradiated and UV-irradiated (450 h) samples. From these spectra, we could not detect any significant

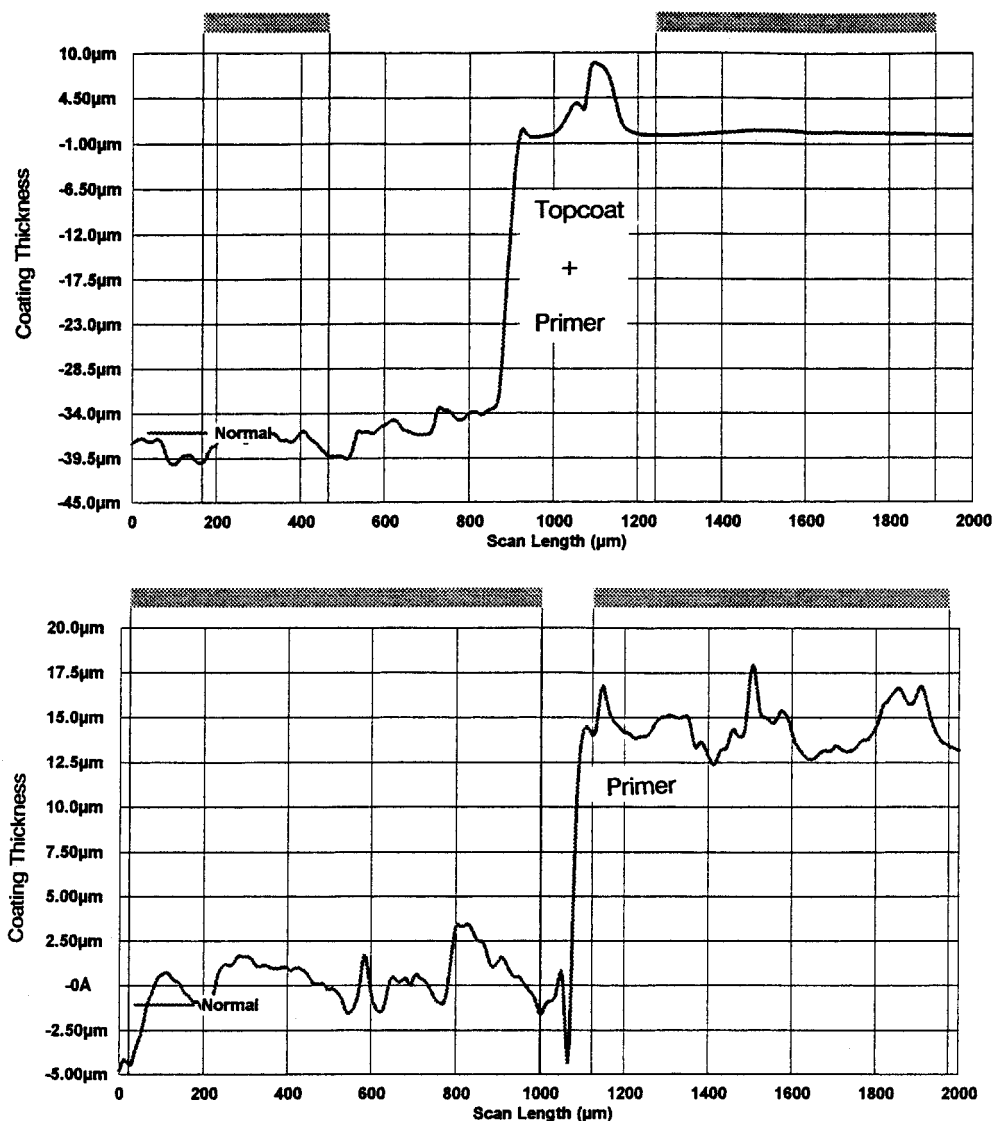


Figure 1. Depth scans of coating (top) and primer (bottom) from profilometry.

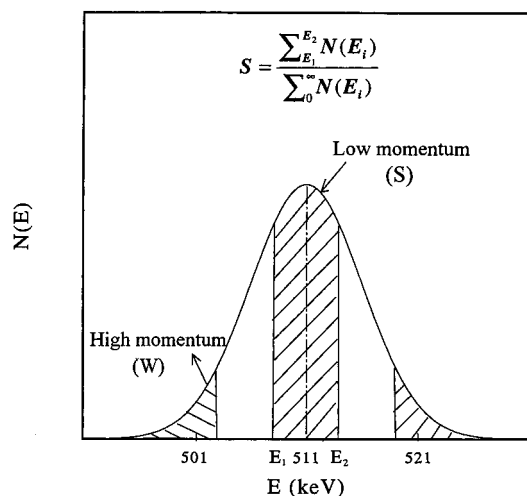


Figure 2. Schematic diagram for defining the S parameter in the DBES spectra from a slow positron experiment.

chemical change in the molecular structure of the coating surfaces due to UV irradiation.

The morphology of the coating surfaces was studied using an AFM (Topometrix TMX 2000). AFM experiments were performed in both paint and pure polyurethane samples at

room temperature under the air. The surface images of paint and pure polyurethane are plotted in Figures 4 and 5, respectively. These results are discussed along with the positron annihilation data in the following sections.

Results and Discussion

When a positron with well-defined energy is injected from a vacuum into a polymer, it either reflects back to the surface or penetrates into the polymer. The fraction of positrons penetrating the polymer substrates increases rapidly as a function of positron energy. The mean implantation depth of the positron as a result of inelastic interactions with polymer molecules is expressed by the formula¹⁴

$$z(E_+) = (40 \times 10^3 / \rho) E_+^{1.6} \quad (2)$$

where z is expressed in nanometers, ρ is the density in kilograms per cubic meter, and E_+ is the incident energy in kiloelectronvolts. For example in a paint sample with a density of $1.5 \times 10^3 \text{ kg/m}^3$, at an energy $E_+ = 1 \text{ keV}$, the positron penetrates 27 nm from the surface.

We performed the DBES experiments as a function of positron incident energy from 0 to 50 keV on paint samples which were exposed to UV irradiation for

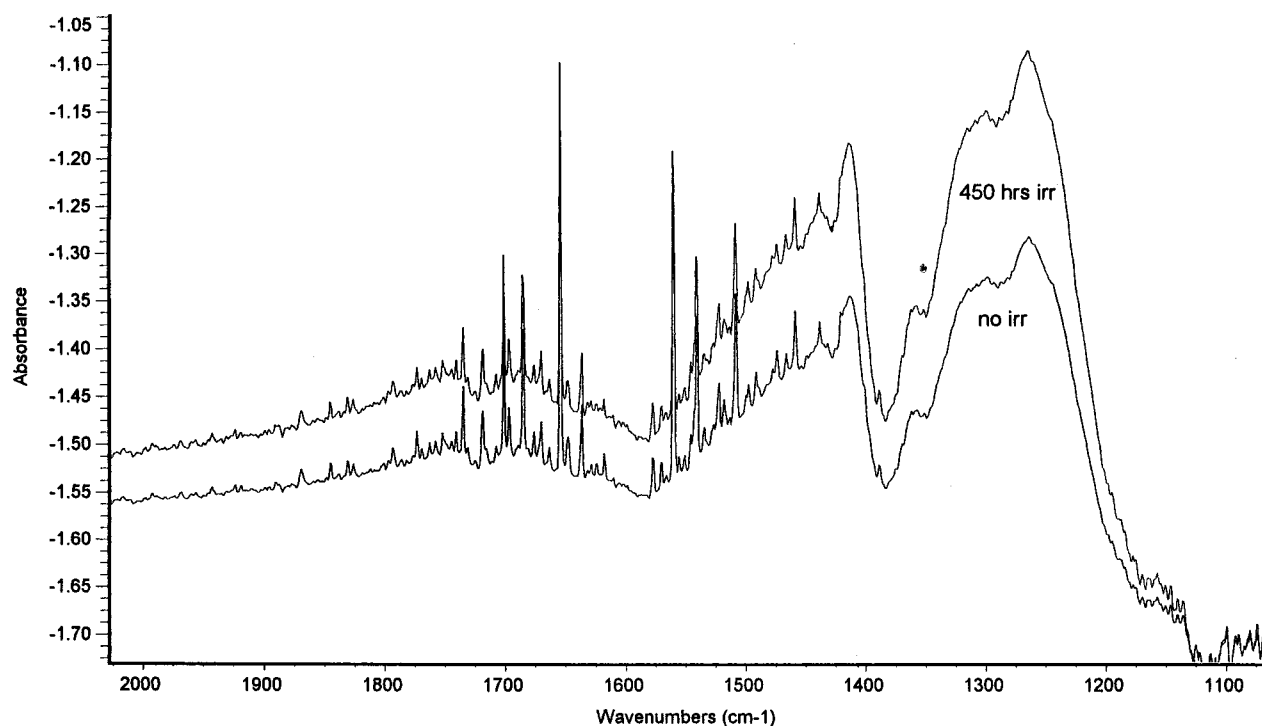


Figure 3. FTIR absorbance for the 450 h UV irradiated (upper plot) and un-irradiated (lower plot) paint samples.

differing periods of time ranging from 0 to 2000 h. Figure 6 shows the S parameter results vs the positron incident energy and the mean depth of penetration for the paint after 0, 207, 404, 1000, and 2000 h of UV irradiation. As shown in Figure 6, S significantly varies as a function of positron incident energy (E_+): (1) at very low energy, S increases as E_+ increases and reaches a maximum at approximately 575 eV (≈ 11 nm); (2) after $E_+ = 575$ eV, S decreases and reaches a minimum at approximately 8 keV ($\approx 0.8 \mu\text{m}$); (3) S then increases to about 20 keV ($3.3 \mu\text{m}$); and finally (4) S remains close to a constant value after 20 keV. Before we discuss these variations, we will describe the processes involved in a positron's interaction with matter when it enters from the vacuum.

(1) Positron and Positronium States in Paints.

After losing their kinetic energy, the positrons penetrating from the vacuum may either directly annihilate with surrounding electrons into two γ -rays or combine with an electron to form a Ps atom. Ps formation is particularly important in polymeric and molecular materials but usually does not exist in oxides, semiconductors, or metals. Ps can be formed on most surfaces. There are two states of Ps: the singlet spin state, called para-positronium (p-Ps), and the triplet spin state, called ortho-positronium (o-Ps). The formation probability for these two states is 1:3. Although o-Ps has a longer lifetime in molecular substrates, neither its three-photon nor two-photon pick-off annihilation contribute much to the current S parameter of DBES. Therefore, only the p-Ps part of Ps annihilation contributes to the S parameter of the DBES spectra, as shown schematically in Figure 2.

When p-Ps is localized in a defect with a dimension (Δx), the momentum (Δp) has a dispersion according to the Heisenberg uncertainty principle, $\Delta x \Delta p \geq h/4\pi$. The S parameter from DBES spectra is a direct measure of the quantity of momentum dispersion (Figure 2). Therefore, in a system with defects, the S parameter is a

qualitative measurement of the defect size and of defect concentration of the materials under investigation. The value of the S parameter also depends on the momentum of the valence electrons which annihilate with the positron. For example, in a paint sample containing TiO_2 , its S parameter will be a small value because Ti contains high-momentum d electrons. We have measured the S parameter of TiO_2 powders as a function of E_+ . The results are shown in Figure 7. As expected, the S parameter in the bulk of TiO_2 (0.404 at 50 keV of Figure 7) is significantly smaller than that of the paint (0.477 at 50 keV of Figure 6).

On the other hand, the S parameter is also directly affected by the Ps and positron diffusion behaviors near the surface. Although both the positron and Ps are known to localize in any defects, such as holes and free volumes,¹³ certain fractions of them may diffuse back to the surface and escape to the vacuum. A complete interpretation of the variation of S parameter vs E_+ will depend on both positron and Ps behaviors and physical properties (mainly defects) of the paints under investigation.

(2) Depth Profile Analysis. Increasing S parameters as shown in Figure 6 are typical for slow positron data near the surface of polymers which contain a large fraction of sub-nanometer defects.^{16,17} As the positron penetrates further into the bulk, an increased Ps formation is also expected, mainly contributed to the S parameter from p-Ps annihilation in polymers. On the other hand, the S parameters decrease in solids which do not contain a large fraction of defects, such as oxides or semiconductors.^{14,18} This occurs because as the positron energy increases, there is a decrease in free Ps escaping from the surface. This is seen in the case of TiO_2 (Figure 7).

Although the topcoat of a paint contains pigments and other additives, we attribute the increase in S vs E_+ (Figure 6) near the surface to the existence of a thin polymer layer, because its variation is similar to the

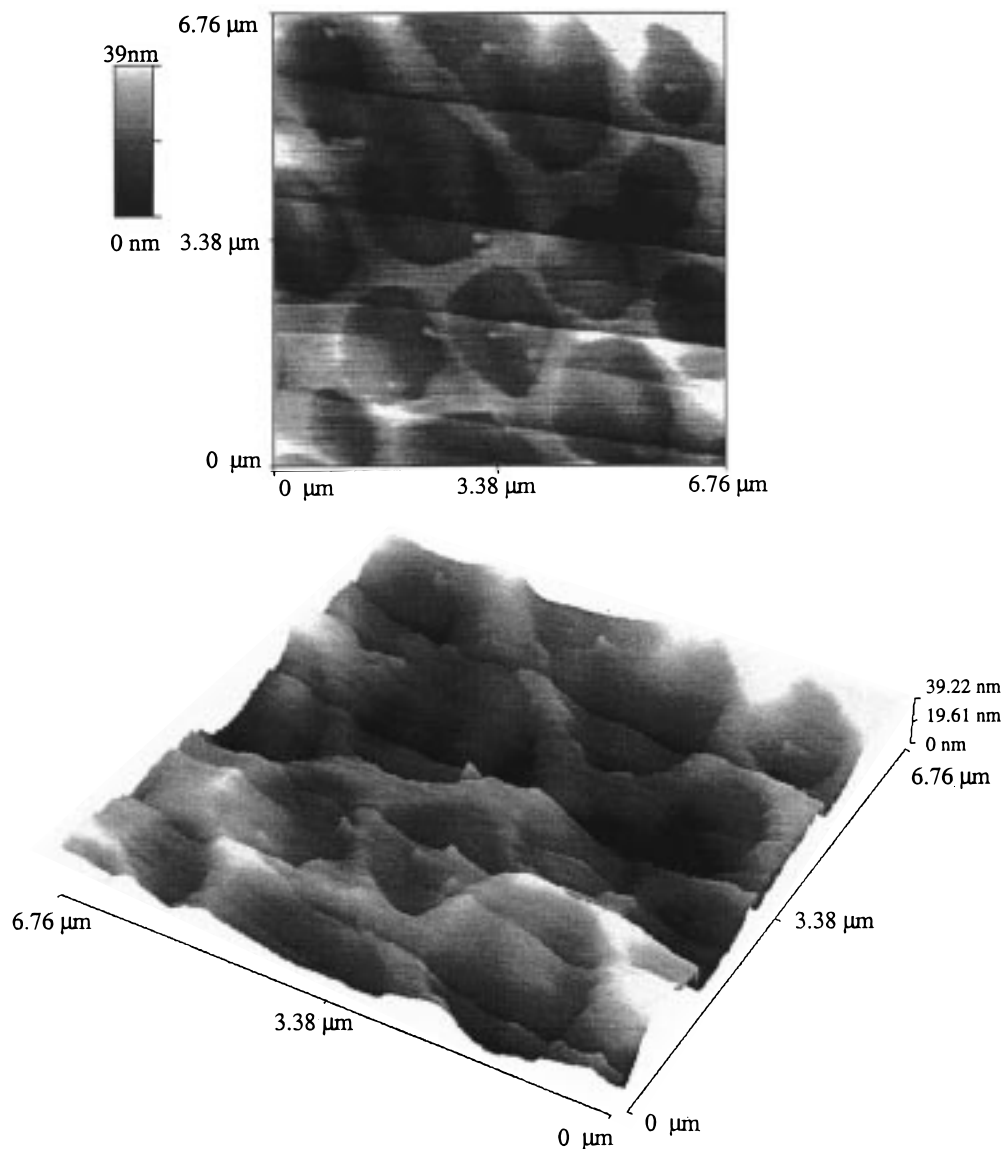


Figure 4. Surface images of AFM in a paint sample studied.

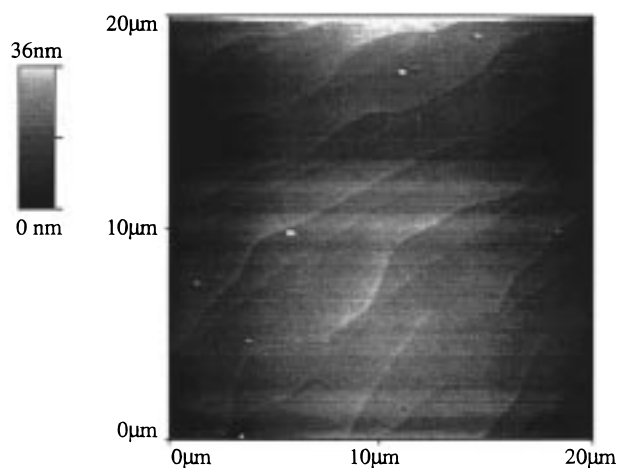


Figure 5. Surface image of AFM in a polyurethane polymer.

surface of a pure polymer.^{16,17} To verify this, we performed an S parameter vs positron incident energy experiment on a pure polyurethane polymer with chemical composition similar to that in our study. The variation of S is plotted in Figure 8 for comparison with the paint data. As shown in Figure 8, the S data near

the surface below 400 eV coincide nicely with the paint data. This is strong evidence that the surface of the paint is a thin polymer layer. The effect of pigment starts to be seen from a depth of approximately 8 nm where, as seen in Figure 8, a decrease of S begins following 500 eV of incident energy, while in pure polyurethane S continues to increase and then remains constant. A valley in S between 500 and 11 keV between 5 nm and 1 μm from the surface indicates a slightly higher composition of TiO_2 than that in the bulk (> 11 keV). This observation is consistent with a previous study on a paint sample having no pigment where a smooth increase of the S parameter was seen.¹⁵ In that study, an S parameter variation similar to ours (Figure 6) was also reported in a paint with pigment.

From the variations of the S parameter (Figures 6–8), we proceed to estimate the depth of the polymer skin layer near the surface using a depth profile analysis method established from positron studies in solids. We employed the VEPFIT software program which decomposes the S parameter into a multilayer model.¹⁹ The results show that one-layer and three-layer models are most suitable for the pure polyurethane and paint samples, respectively. The results of diffusion coef-

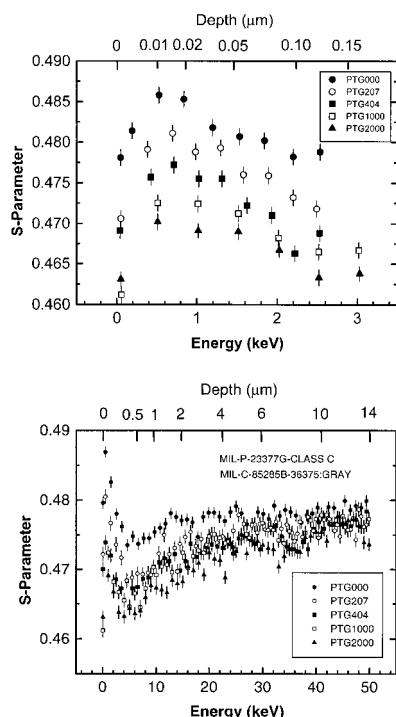


Figure 6. *S* parameters vs positron incident energy in a coating system. The number after PTG (paint/gray color) refers to the number of hours of UV irradiation.

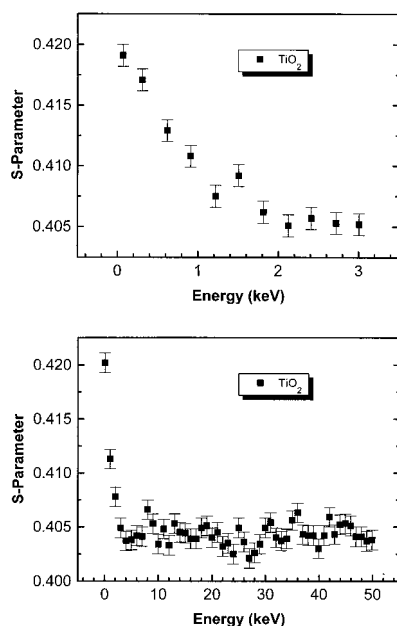


Figure 7. *S* parameters vs positron incident energy for a powder TiO_2 sample.

ficients and the location of layer boundaries are listed in Table 1 and shown in Figure 8.

Two diffusion lengths in polyurethane are obtained from one-layer analysis, $L_1 = 4 \pm 1.2$ nm and $L'_1 = 56 \pm 12$ nm, which corresponds to the Ps and the positrons, respectively. Similar diffusion lengths (3.3 ± 1.0 and 3.0 ± 1.5 nm) at short ranges near the surface are obtained for both un-irradiated and UV-irradiated paint samples from the three-layer model. They are close to the diffusion length of Ps in pure polyurethane. The first boundary distances from VEPFIT are 11 ± 1.0 nm and 10 ± 1.0 nm from the surface in un-irradiated and irradiated paint samples, respectively. The second

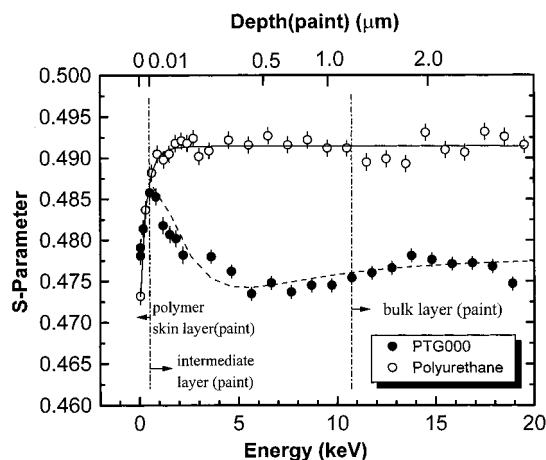


Figure 8. *S* parameters vs positron energy in pure polyurethane and in a paint. Dashed vertical lines indicate the location of layer boundaries for the paint sample (PTG) according to the VEPFIT fitted results (lines drawn).

Table 1. Multilayer Analysis of Coating Systems and Polyurethane^a

samples	L_1 (nm)	D_{Ps} (10^{-5} cm^2/s)	L'_1 (nm)	D_+ (10^{-2} cm^2/s)	L_2 (μm)	D_2 (cm^2/s)
polyurethane	4.0 ± 1.2	1.3	56 ± 12	1.3		
paint (un-irradiated)	3.3 ± 1.0	1.1			0.72 ± 0.12	0.43
paint (2000 h irradiation)	3.0 ± 1.5	1.0			0.70 ± 0.11	0.41
TiO_2 (powder)					0.26 ± 0.10	0.28

^a L_1 , L'_1 , L_2 are the resulting diffusion lengths of Ps and the positron from fitted *S* parameters using VEPFIT. D_{Ps} , D_+ , D_2 are the calculated diffusion coefficients of Ps and the positrons near the surface of polymers and the positrons in the bulk of the paint, respectively, according to eq 3 and L_1 , L'_1 , and L_2 data.

diffusion lengths in paints are 0.7 ± 0.1 μm . Due to the limited fitting power of the VEPFIT program, the longer diffusion length of positrons in the polymer skin near the surface (L'_1) is not resolvable in the paint data. The second boundaries are found to be at 1.2 ± 0.1 μm from the surface for the un-irradiated and irradiated paint samples, respectively, according to the VEPFIT outputs.

The interpretation of these two distances is as follows: (1) the paint samples have a polymer skin surface which is approximately 10 nm thick, and (2) ≈ 1 μm features are consistent with the size of TiO_2 particles. This is supported from the surface images obtained by the AFM as shown in Figures 4 and 5. In Figure 4, there exists an image (circle shape) of a particle size on the order of micrometers, which is about the size of TiO_2 pigment particles. This corresponds to the second boundary length as determined by the VEPFIT analysis on *S* variations. The uneven height of the paint surface (Figure 4) as shown from AFM was found to be ≈ 1 –40 nm. This is not seen in a pure polyurethane surface (Figure 5). The height of the paint structure is within the range of the first skin depth analyzed from the positron data. From these data on the depth profile of the topcoat in the paint under study we conclude that (1) there exists approximately 10 nm of polymer skin from the surface of the paint, (2) inside the polymer skin there exists an intermediate transition layer (approximately 1 μm) where TiO_2 (size $\approx \mu\text{m}$) starts to disperse with the polymers and other additives, and (3) inside the transition layer there exists the bulk layer of paint.

This assignment is shown in Figure 8 where dashed vertical lines represent the two boundaries among three layers in the paint.

From the obtained diffusion lengths, we proceed to estimate the Ps and positron diffusion coefficients in coating systems which have not been reported in the literature. The probability of positrons and Ps annihilating in a polymer depends on their diffusion coefficients. The mean diffusion length (L) of the positron or Ps undergoing three-dimensional Brownian motion can be expressed as¹²

$$L = [6\tau D]^{1/2} \quad (3)$$

where D and τ are the Ps or positron diffusion coefficient and their lifetime, respectively. For a polymer which contains a large fraction of defects, i.e., holes, free volumes, and interfaces, the D for Ps (D_{Ps}) is expected to be much smaller than that for the positron due to its localization, neutral charge, and high polarizability. Typical values of D_{Ps} in polymers for Ps are known to be a few 10^{-6} cm²/s,²⁰ while the corresponding diffusion coefficients for the positron (D_+) are on the order of 10^{-2} cm²/s.^{12,14} For example, D_{Ps} for polystyrene was reported to be 3×10^{-6} cm²/s and $\tau = (2-3) \times 10^{-9}$ s.²⁰ Our calculated results based on the measured Ps and positron lifetimes in bulk polyurethane (2.23 ns), paints (2.10 ns), and TiO₂ (0.41 ns) are also listed in Table 1. The small diffusion coefficients of Ps (10^{-5} cm²/s) and the positron (10^{-2} cm²/s) in polyurethane are consistent with the existing results in polymers.²⁰

(3) UV Irradiations. One of the most interesting results in DBES studies of coatings is an S parameter decrease when the samples are subjected to UV irradiation, as shown in Figure 6 and reported by others.¹⁵ In this work, we performed a systematic study of the effect of UV irradiation on coating samples under a controlled environment. The S parameters vs energy for four different periods of UV irradiation have been plotted in Figure 6. As shown, the S parameters systematically decrease as a function of duration of UV irradiation. Before we proceed to interpret these changes as an effect of UV irradiation, we examine the possibility of a thermal effect occurring concurrently with the UV irradiation.

We have performed S parameter experiments on a series of identical batches of samples exposed to the same environment except for being kept in darkness. The results from these samples reveal no significant difference in S parameters between the sample annealed at 45 °C for 600 h in the dark and the original un-exposed samples. With these results, we exclude the thermal effect as a cause of decreased S parameter. We then proceed as follows to interpret the decrease in the S parameter due to UV irradiation.

When UV light shines on a paint sample, it penetrates into the paint and the absorbance attenuates as a function of depth. The UV absorption spectra show significant UV absorption into the depth on the order of micrometers. To quantitatively interpret the results, we calculated the change of S parameters between the un-irradiated and irradiated samples as

$$\Delta S = S_0 - S_n \quad (4)$$

where S_0 and S_n are the S parameter for the samples without and with n hours of UV irradiation, respectively. Figure 9 shows the variations of ΔS vs the

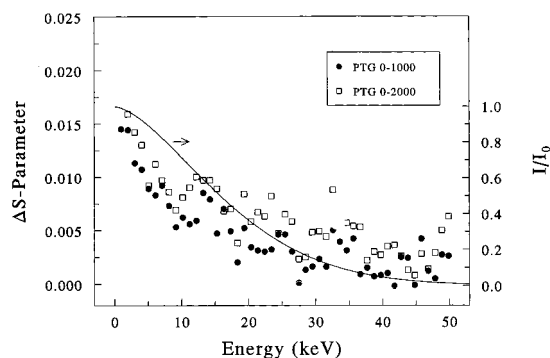


Figure 9. Difference of S parameter between UV-irradiated and un-irradiated paint samples for 1000 and 2000 h of irradiation. ΔS is defined in eq 4. The line represents the UV transmittance curve according to Beer's law.

positron incident energy (only those data from 500 eV and higher) for samples irradiated for 1000 and 2000 h. It is seen that the change of S is greater near the surface and it decreases as the positron penetrates into the bulk from the surface. This is expected from the attenuation of UV transmittance as a function of depth, as shown in the decrease of UV transmittance vs depth. In Figure 9, we also plot the decrease of UV transmittance vs positron energy as calculated from eq 2. Good agreement between UV transmittance and ΔS vs E_+ is clearly seen in Figure 9. Therefore, we attribute the decrease of S parameter to UV irradiation.

There are several possible causes for a decrease in S due to UV irradiation as shown in Figure 9. Two fundamental effects—chemical and physical—may be due to interactions between UV irradiation and coating systems. The chemical effect may result from the decomposition of chemical bonds and formation of free radicals. The breaking of a chemical bond may be monitored by measuring the molecular spectra near the surface. However, as shown in Figure 3, there is no detectable difference in the FTIR spectra between the un-irradiated paint samples and samples irradiated for 450 h. It implies that if there is a broken chemical bond, the effect is not detectable by FTIR, which probes the molecular structure near the surface (nm).

The next possible effect is the formation of radicals due to UV irradiation. This effect is more important in organic polymers than inorganic pigments. We have tried to observe long-lived free radicals by measuring the electron spin resonance (ESR) spectra on these samples using a Bruker ESR spectrometer to compare with current PAS results. Although there exists a long-lived ESR signal in these samples, the correlation between these long-lived ESR signals and ΔS is yet to be investigated further. This is understandable because most free radicals from UV irradiation are short-lived. On the other hand, we have observed a short-lived free radical signal after UV irradiation. The short-lived free radical data should shed more light on the initial stage of radical formation due to UV irradiation. An in situ experiment is in progress in which S parameter data are being collected as a function of UV irradiation. These results will be reported with the ESR data in the future.

Considering a simplified picture of the effects of UV degradation on the paint as described above, we proceed to search for possible explanations regarding the kinetics and the mechanism of photodegradation due to UV irradiation. Our first attempt is to examine the change

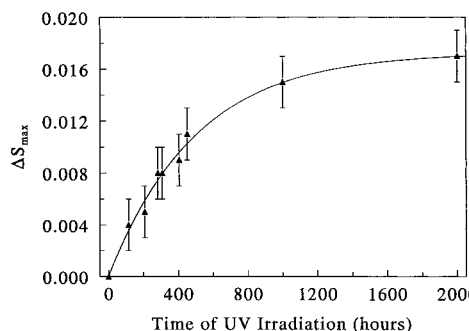


Figure 10. Maximum decrease of S due to UV irradiation vs time in a coating sample. The line presents a fitted rate equation (eq 5) with $\Delta S_{\infty} = 0.0173$ and $k = 0.002 \text{ h}^{-1}$.

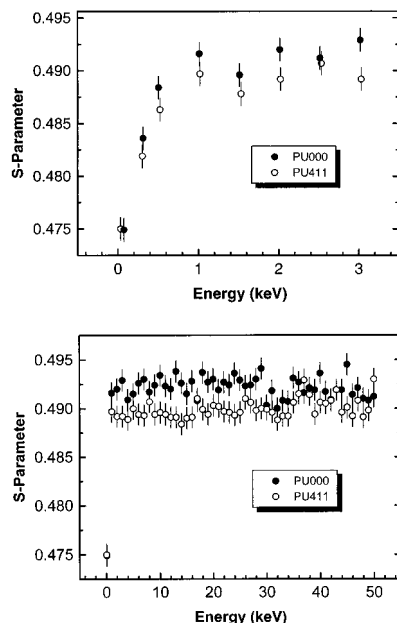


Figure 11. S parameters of pure polyurethane polymers vs positron incident energy. The number after PU refers to the number of hours of UV irradiation.

of ΔS as a function of time of irradiation. As shown in Figure 6, the amount of change in the S parameter is found to be a function of the duration of UV irradiation. In Figure 10, we plot the maximum ΔS (ΔS_{\max}) vs time of UV irradiation, where the positron energy (E_+) corresponding to ΔS_{\max} is found to be 575 eV (independent of the duration of irradiation) from the plots of S vs E_+ (such as those shown in Figure 6). $E_+ = 575 \text{ eV}$ is also identified as the location (11 nm) from the paint surface where the pigment (TiO_2) starts to contribute to the decrease in the S parameter as shown in Figure 6.

The direct relationship between ΔS_{\max} and the duration of UV irradiation (t) is obvious in Figure 10. We attempted to search for kinetics information from ΔS_{\max} vs time of UV irradiation. We fit the data of ΔS_{\max} vs time into a variety of functions and found that an exponential equation such as eq 5 below gives a very good fit, where S_{∞} and k are the fitting parameters and

$$\Delta S_{\max} = \Delta S_{\infty}[1 - e^{-kt}] \quad (5)$$

t is the time expressed in hours. The values of ΔS_{∞} and k which fit best were found to be 0.0173 ± 0.0003 and $0.0020 \pm 0.0001 \text{ h}^{-1}$, respectively. In the kinetics theory, a first-order reaction mechanism has a negative

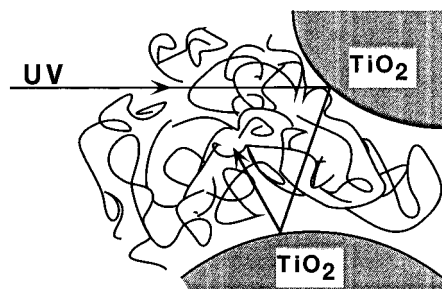


Figure 12. Schematic diagram representing the enhancement of UV photodegradation on polymer chains due to the presence of pigment in a paint.

exponential function between the concentration and time. If we postulate ΔS as a measure of product concentration, the current ΔS results indicate a first-order rate determining step in the reaction mechanism for the degradation due to UV irradiation on the paint samples. Then k is reduced as the degradation rate is expressed in eq 5. From this postulated kinetics, the half-life of the degradation reaction due to UV irradiation is calculated to be 347 h.

Our second attempt is to propose the possible chemical reaction mechanism due to UV irradiation. Since paints are complicated composites, more data will be required on simple and well-defined systems in order to elucidate the UV irradiation effect on different components. Along this line of investigation, we have performed S parameter experiments on a similar polyurethane polymer for both un-irradiated and UV-irradiated (411 h) samples. Figure 11 shows the S parameters vs positron energy in pure polyurethane. It is interesting that we observed a similar trend of decrease in S parameters due to UV irradiation in pure polyurethane samples as occurred in the paint (Figures 6, 9, and 10). Furthermore, from an experiment on a TiO_2 sample, we found no decrease in S at all due to UV irradiation. Since the largest difference in S occurs near the skin surface layer (Figures 6, 9, and 10), we conclude that the degradation effect of UV irradiation is on the polymers of the paint under study here.

Upon examining the amount of ΔS in polyurethane (Figure 11), we find that the effect of UV irradiation is much deeper in the pure polymer than in the paint. For example, at $E_+ = 575 \text{ eV}$ (the ΔS_{\max} in the paint), there is barely a detectable ΔS (< 0.002 in Figure 11) in polyurethane, while in the paint ΔS_{\max} is 0.010 ± 0.002 (Figure 9). On the other hand, the value of ΔS_{\max} for polyurethane after 411 h of irradiation is approximately at $E_+ = 12 \text{ keV}$, which is equivalent to $1.9 \mu\text{m}$ depth from the surface. ΔS_{\max} for polyurethane after 411 h irradiation at $E_+ = 12 \text{ keV}$ reaches 0.005 ± 0.002 , which is about half that of the paint (Figure 8). This indicates that the effect of UV irradiation on the paint is more severe than on the pure polymer. One plausible explanation is that the microstructure of the interfaces and boundaries between the polymer and pigments enhances the degradation processes due to the reflection of the UV light from the TiO_2 particles. This enhancement of UV degradation on polymers due to the presence of TiO_2 in the paint is schematically shown in Figure 12. From the ΔS data, we estimate the enhancement factor due to pigment to be approximately 2.

The third attempt is to propose a mechanism involving morphological change due to UV irradiation, which is an intriguing problem in the coating industry.²¹ The

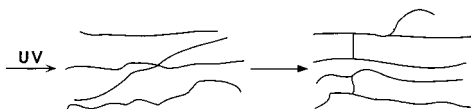


Figure 13. Schematic diagram representing a mechanism of photodegradation of polymer chains due to UV irradiation.

decrease in S parameter indicates a decrease of either defect size or concentration due to irradiation. As mentioned before, the sensitive region of defect size is on the order of 0.2–2 nm, as determined by the positron annihilation method.¹³ Polymer chains break when irradiated, which results in decreased polymer end-to-end length.²¹ The currently used polyurethane is a cross-linked polymer.²² Here we propose a mechanism in which chains are broken and the cross-linking density of polyurethane is subsequently increased. This proposed mechanism is schematically shown in Figure 13.

According to this mechanism, UV irradiation introduces a local structural change, which is sensitive to the observed S parameter of DBES. The S parameter is particularly sensitive to the change of sub-nanometer hole and free-volume change.¹³ The S parameter is particularly sensitive to the resulting cross-link density change due to UV irradiation. According to a systematic positron annihilation study of epoxy polymers, a polymer with a higher cross-link density shows a smaller value of free-volume hole size and fraction.²³ In the case of UV irradiation on polymers as schematically shown in Figure 13, it leads to an increase of cross-linking density, or a decrease in free volume, hole fraction and size. This effect results in a decrease in the S parameter due to UV irradiation, as shown in Figures 6 and 9–11.

Furthermore, in polymeric materials, a reduction of free-volume concentration is expected to lead to a loss of mechanical properties, such as modulus, toughness, etc. The above proposed mechanism is consistent with the loss of polymer durability as a result of degradation of the coating by UV irradiation. The current positron annihilation data support this free-volume concept in the interpretation of the degradation process of paint materials.

Conclusion

A study of UV irradiation in aircraft coating systems has been reported using positron annihilation spectroscopy. We interpret the variation of S parameter as an indicator for the existence of a polymer skin layer (11 nm) and a transition layer (1.2 μm) into the bulk of paints. The decrease of the S parameter due to UV irradiation is interpreted as resulting from degradation of polymer chains leading to an increase in the cross-linking density. Our study detected enhanced degradation due to the presence of TiO_2 and the subsequent loss of free-volume and hole fraction due to UV irradiation. The current results demonstrate a new approach for investigating the origin of degradation and the initiation of atomic level defects using the S parameter of Doppler energy spectra.

Acknowledgment. We are especially thankful to Dr. Da-Ming Zhu for helping prepare the AFM experiments, to Dr. A. Mitra for FTIR experiments, and to Dr. T. F. Thomas for UV experiments. This research has been supported by the Air Force Office of Scientific Research under Contract No. F49620-97-1-0162 (University of Missouri—Kansas City) and the Department

of Energy (Brookhaven National Lab) under Contract No. DE-AC02-76-CH0016.

References and Notes

- (1) For examples, see: Dickie, R. A. *Prog. Org. Coat.* **1994**, *25*, 3; Dickie, R. A. In *Organic Coatings: Science and Technology*; Wicks, Z. W., Jr., Jones, F. N., Pappas, S. P., Eds.; Wiley: New York, 1994; Vols. I and II.
- (2) *Concept of Operations for an Air Force Coating Technology Integration Office*; U.S. Department of the Air Force: Washington, DC, Jan 31, 1995.
- (3) For example, see: *Advances in Coating Technologies for Corrosion- and Wear-Resistant Coatings*; Srivatsa, A. R., Clayton, C. R., Hirvonen, J. K., Eds.; Minerals, Metals, and Materials Society: Warrendale, PA, 1995.
- (4) For examples, see: *Polymer Durability: Degradation, Stabilization, and Lifetime Prediction*; Clough, R. L., Billingham, N. C., Gillen, K. T., Eds.; Advances in Chemical Series 249; American Chemical Society: Washington, DC, 1996. Schnabel, W. *Polymer Degradation, Principles and Practical Applications*; Hanser Gardner: Cincinnati, OH, 1982.
- (5) For example, see: *Industrial Coatings: Properties, Applications Quality, and Environmental Compliance. Proceedings of the Advances in Coatings Technology Conference*, Chicago, Illinois, November 1992; ASM International: Materials Park, OH, 1992.
- (6) For example, see: *Polymer Spectroscopy*; Fawcett, A. H., Ed.; Wiley: New York, 1996.
- (7) For example, see: *Multi-Dimensional NMR, FT-IR/Raman, and Fluorescence Spectroscopies*; Urban, M. W., Provder, T., Eds.; ACS Symposium Proceedings Series 598; American Chemical Society: Washington, DC, 1995.
- (8) For example, see: *Vibrational Spectroscopy of Molecules and Macromolecules on Surfaces*; Urban, N. W., Ed.; Wiley-Interscience: New York, 1993.
- (9) For example, see: *Multidimensional Solid-State NMR and Polymers*; Schmidt-Rohr, K., Spiers, H. W., Eds.; Academic Press: San Diego, CA 1994.
- (10) For example, see: Gerlock, J. L.; Bauer, D. R.; Mielewski, D. F. *Proc. 18th Int. Conf. Org. Coat. Sci. Technol.* **1992**, *225*.
- (11) For example, see: *Polymer Characterization*; Hunt, B. J., James, M. I., Eds.; Blackie Academic and Professional: London, 1993.
- (12) For examples, see: *Positron Spectroscopy of Solids*; Dupasquier, A., Mills, A. P., Jr., Eds.; IOS: Amsterdam, 1995. *Positron and Positronium Chemistry*; Schrader, D. M., Jean, Y. C., Eds.; Elsevier: Amsterdam, 1988.
- (13) For example, see: Jean, Y. C. In *Positron Spectroscopy of Solids*; Dupasquier, A.; Mills, A. P., Jr., Eds.; IOS: Amsterdam, 1995; p 503.
- (14) Schultz, P. J.; Lynn, K. G. *Rev. Mod. Phys.* **1989**, *60*, 701.
- (15) Hulett, L. D., Jr.; Wallace, S.; Xu, J.; Nielson, B.; Scales, C.; Lynn, K. G.; Pfau, J.; Schaub, A. *Appl. Surf. Sci.* **1995**, *85*, 334.
- (16) Kobayashi, Y.; Kojima, I.; Hishita, S.; Suzuki, T.; Asari, E.; Kitajima, M. *Phys. Rev. B* **1995**, *52*, 823.
- (17) Jean, Y. C.; Zhang, R.; Cao, H.; Yuan, J.-P.; Huang, C. M.; Nielsen, B.; Asoka-Kumar, P. *Phys. Rev. B* **1997**, *56*, R8459.
- (18) Suzuki R.; Kobayashi, Y.; Mikado, T.; Ohgaki, H.; Chiwaki, M.; Yamazaki, T.; Tomimasu, Y. *Jpn. J. Appl. Phys.* **1991**, *30*, L532.
- (19) van Veen, A.; Schut, H.; de Vries, J.; Hakvoort, I.; Jpma, M. R. In *American Institute Physics Conference Proceedings*; Schultz, P. J., Massoumi, G., Simpson, P. J., Eds.; American Institute of Physics: New York, 1990; Vol. 218, p 171.
- (20) Hirata, K.; Kobayashi, Y.; Ujihira, Y. *J. Chem. Soc., Faraday Trans.* **1996**, *92*, 985.
- (21) For examples, see: *Irradiation of Polymers: Fundamentals and Technological Applications*; Clough, R. L., Shalaby, S. W., Eds.; ACS Symposium Series 620; American Chemical Society: Washington, DC, 1996. *Radiation Effects on Polymers*; Clough, R. L., Shalaby, S. W., Eds.; ACS Symposium Series 475; American Chemical Society: Washington, DC, 1991.
- (22) For examples, see: *Resins for Coatings*; Stole, D., Freitag, W., Eds.; Hanser Gardner: Cincinnati, OH, 1996. *Polyurethane Handbook*, 2nd ed.; Oertel, G., Ed.; Hanser Gardner: Cincinnati, OH, 1993.
- (23) Jean, Y. C.; Sandreczki, T. C.; Ames, D. P. *J. Polym. Sci., Polym. Phys. Ed.* **1986**, *24*, 1247.

MA9802778